

## THE DETECTION OF $^{13}\text{C}$ O AND OTHER APPARENT ABUNDANCE ANOMALIES IN THE SECONDARY STARS OF LONG-PERIOD CATAclySMIC VARIABLES

THOMAS E. HARRISON<sup>1,2</sup> AND HEATHER L. OSBORNE<sup>2</sup>

Department of Astronomy, New Mexico State University, 1320 Frenger Mall, Las Cruces, NM 88003-8001; tharriso@nmsu.edu, hosborne@nmsu.edu

AND

STEVE B. HOWELL

WIYN Observatory and National Optical Astronomy Observatory, 950 North Cherry Avenue, Tucson, AZ 85726; howell@noao.edu

Received 2003 October 15; accepted 2004 February 18

### ABSTRACT

We present moderate-resolution ( $R > 1800$ ) infrared  $K$ -band spectra of 12 long-period ( $P_{\text{orb}} > 6$  hr) cataclysmic variables (CVs). We detect absorption lines from the photospheres of the secondary stars in every system, even though two of them were undergoing outbursts. We have attempted to assign a spectral type to each of the secondary stars, and these classifications are generally consistent with previous determinations. We find evidence for abundance anomalies that include enhancements and/or deficits for all of the species commonly found in  $K$ -band spectra of G- and K-type dwarfs. There is, however, only one common abundance anomaly: extremely weak CO features. Only two of the 12 objects appeared to have normal levels of CO absorption. We interpret this as evidence of low carbon abundances. In addition, we detect  $^{13}\text{C}$ O absorption in four of the 12 objects. Depleted levels of  $^{12}\text{C}$  and enhanced levels of  $^{13}\text{C}$  indicate that material that has been processed in the CNO cycle is finding its way into the photospheres of CV secondary stars. In systems with luminous accretion disks, we find that the spectrum of the secondary star is contaminated by a source that flattens (reddens) the continuum. While free-free or classical accretion disk spectra are flatter than the blackbody-like spectra of G and K dwarfs, removal of such contamination from the  $K$ -band data results in spectra in which the absorption features become too strong to be consistent with those of G and K dwarfs.

*Key words:* infrared: stars — novae, cataclysmic variables

### 1. INTRODUCTION

Cataclysmic variables are short-period binary systems consisting of a white dwarf primary that is accreting material via Roche lobe overflow from a low-mass, late-type secondary star. The commonly proposed evolutionary history for cataclysmic variables (CVs) establishes that the vast majority of CV secondary stars have undergone very little evolution during their lifetime (see Howell, Nelson, & Rappaport 2001 and references therein). The formation of a CV from a wide binary containing two main-sequence stars is envisaged to have three main phases: First, the orbital separation of the wide binary of the pre-CV is rapidly shrunk in a common-envelope phase during which the secondary star orbits inside the red giant photosphere of the white dwarf progenitor. The second phase is a very long epoch in which gravitational radiation, or a magnetically constrained wind from the secondary star (“magnetic braking”), extracts angular momentum from the binary, resulting in the eventual contact of the photosphere of the secondary star with its Roche lobe. The final phase begins once the secondary star contacts its Roche lobe, mass transfer to the white dwarf is initiated, and all of the phenomena associated with CVs are observed. During the lifetime of the mass transfer phase, the overall mass of the

secondary star is gradually reduced. Much of the material accreted by the white dwarf is believed to be lost from the typical CV system through numerous classical nova eruptions. In both the common-envelope phase and during classical nova eruptions, material with a peculiar composition can be deposited in the photospheres of CV secondary stars.

Evidence for the existence of peculiar abundance patterns in CVs is growing. For example, using UV spectroscopy, Cheng et al. (1997) found that the carbon abundance was 5 times solar, nitrogen was 3 times solar, and silicon was less than 0.1 times solar for the white dwarf in WZ Sge. They suggested that this material was probably transferred from the secondary star. For VW Hyi, Sion et al. (1997) found that the white dwarf appeared to be deficient in carbon (0.5 times solar), iron (0.5 times solar), and silicon (0.1 times solar) but had an excess of nitrogen (5 times solar), oxygen (2 times solar), and phosphorus (900 times solar). Sion et al. (2001) found subsolar abundances for carbon (0.05 times solar) and silicon (0.1 times solar) for the white dwarf in RX And. In both CN Ori (Urban et al. 2000) and AH Her (Lyons et al. 2001), subsolar silicon abundances were found. Meanwhile, Sion et al. (1998) and Long & Gilliland (1999) estimated that the carbon abundance of the white dwarf in U Gem is about 0.1 times solar, while the nitrogen abundance is about 4 times solar. Harrison et al. (2000) found from infrared spectroscopy that the secondary star in U Gem appeared to have extremely weak CO features, suggesting it was deficient in either carbon or oxygen. If so, the deficit of carbon on the white dwarf for U Gem could be easily explained by the transfer of carbon-poor material from the secondary star. In addition, Harrison et al. found that the secondary star of SS Cyg displayed

<sup>1</sup> Visiting Astronomer, Cerro Tololo Inter-American Observatory, National Optical Astronomy Observatory, which is operated by the Association of Universities for Research in Astronomy, Inc., under cooperative agreement with the National Science Foundation.

<sup>2</sup> Visiting Astronomer at the Infrared Telescope Facility, which is operated by the University of Hawaii under contract from the National Aeronautics and Space Administration.

weaker CO features than it should for its spectral type, along with an apparent magnesium deficit. Mennickent & Diaz (2002) report weak CO absorption for the late-type secondary in VY Aqr. It appears that the both the primary and secondary stars in CVs have peculiar compositions.

Recently, Gänsicke et al. (2003) have reported on anomalous N  $\nu$ /C IV line flux ratios in new *Hubble Space Telescope* (HST) STIS ultraviolet spectroscopy for several CVs and compiled a list of 10 CVs that all show similar spectra. They conclude that these represent true abundance anomalies, and that nitrogen is strongly enhanced relative to carbon.

What could be the origin of such abundance anomalies? Sion (1999) suggests the abundance anomalies in the white dwarf photospheres may result from the nuclear processing in classical nova explosions. As shown by José, Coc, & Hernanz (2001), however, only classical novae with very massive white dwarfs ( $\sim 1.35 M_{\odot}$ ) can produce nuclei such as silicon or phosphorous in thermonuclear burning (and such burning increases, not decreases, the abundance of silicon). White dwarf masses in typical CV systems cluster near  $0.6 M_{\odot}$ . The presence of similar abundance patterns in the secondary stars suggests that for most CVs they are a more likely source for material of peculiar composition. Marks & Sarna (1998) performed a detailed theoretical study of the possible effects on the surface abundances of the secondary star due to both evolutionary effects in the secondary itself and sweeping up of common-envelope (CE) material or matter accreted from classical nova ejecta. All such events could place thermonuclear-processed material into the photosphere of the secondary star. Considering the first case, Marks & Sarna find that the photospheric chemistry of the secondary star could show large abundance variations in carbon, nitrogen, and oxygen from evolutionary effects alone. In this scenario, the CNO tri-cycle is operating in the secondary star either before or during the contact phase. As material is removed from the secondary star, layers where the CNO tri-cycle was operating are exposed, or mixed to the surface, creating abundance and isotopic variations in CNO species. Especially relevant are their predictions of an overall deficit in carbon, enhancements in nitrogen, and a dramatic change in the ratio of  $^{12}\text{C}$  to  $^{13}\text{C}$ . For this work, however, Marks & Sarna only considered initially massive secondary stars ( $1.0\text{--}1.5 M_{\odot}$ ), whereas Howell et al. (2001) have shown that massive secondaries are likely to be present in only a small fraction of CVs.

Marks & Sarna (1998) also performed a study of the effects on the surface abundances of the secondary star due to sweeping up of CE material or by accreting classical nova ejecta. They concluded that any material acquired during the CE phase would be thoroughly mixed into the secondary star during the extended period between the CE phase and the time the secondary contacted its Roche lobe. Marks & Sarna did find that if the process of accreting nova ejecta was efficient, dramatic abundance and isotopic anomalies could be present in the photospheres of CV secondaries.

Gänsicke et al. (2003) suggest that the anomalous nitrogen-to-carbon abundances are a natural consequence of a scenario in which the initial mass of the current donor star is greater than that of the white dwarf. As described by Schenker et al. (2002), in this situation a short-lived phase of very high, and dynamically unstable, mass transfer quickly whittles away the outer layers of the donor star, leading to the production of a CV with a relatively normal mass ratio, but one where the donor star is now the CNO-processed core of the massive donor. Schenker et al. propose that the unusual CV system

AE Aqr has just completed this phase of evolution. As shown in their Figure 9, the surface chemical abundance ratios of  $^{12}\text{C}/^{13}\text{C}$  and C/N drop by 1 or 2 orders of magnitude as a system like AE Aqr evolves to become a CV. This scenario predicts depleted levels of carbon, enhanced levels of nitrogen and  $^{13}\text{C}$ , and that the donor stars will have spectral types that are too late for their orbital periods.

Thus, the detection and measurement of abundance anomalies in a secondary star may provide direct insight into the evolutionary history of a CV. Of course, it remains quite possible that any observed abundance anomalies might arise because of unusual excitation conditions within the nonequilibrium photospheres of irradiated, mass-losing secondary stars. We present new infrared spectra of a dozen long-period cataclysmic variables to search for additional abundance anomalies in their secondary stars. We detect the secondary star in every CV and find evidence for carbon deficits in nearly all of them. In addition, we detect  $^{13}\text{CO}$  for the first time in a CV secondary star. We find that in the case of MU Cen, the strength of the  $^{13}\text{CO}$  feature suggests that the CNO cycle has run to completion ( $^{12}\text{CO}/^{13}\text{CO} = 3.2$ ). We also find a wide range in the strengths of lines from such elements as sodium, calcium, magnesium, silicon, and iron when compared with main-sequence stars of the *most appropriate* spectral type. The origin of such a wide range of behavior is not easily identifiable. The detection of enhanced  $^{13}\text{CO}$  certainly suggests that CNO-processed material has made it into the atmospheres of a number of CV secondary stars, but whether this is from the accretion of material, or due to the evolutionary history of the secondary star itself, remains unclear. Further high-resolution, high signal-to-noise ratio (S/N) spectroscopic observations will be needed to quantify these anomalies. Equally important, however, will be the need for good atmosphere models to help rule out any effects due to peculiar excitation conditions.

In the next section we discuss our observations, followed by a description of the spectra of the objects in § 3, followed by our conclusions in § 4.

## 2. OBSERVATIONS

Infrared spectroscopy for the program objects was obtained using SpeX<sup>3</sup> on the Infrared Telescope Facility (IRTF) on Mauna Kea, and at the Cerro Tololo Inter-American Observatory using OSIRIS<sup>4</sup> on the 4 m Blanco Telescope. The observing run with OSIRIS occurred on 2002 March 20 and 21. There were two different observing runs with SpeX: 2002 April 6 and 7 and 2003 May 16–19. Both instruments were used in the mode that provided the highest possible resolution in the *K* band. For SpeX, this consisted of using the spectrograph in single-order mode with a  $0''.3$  slit, giving a dispersion of  $5.51 \text{ \AA pixel}^{-1}$ . The spectra produced in this mode covered the entire *K* band, from  $1.96$  to  $2.50 \mu\text{m}$ . OSIRIS was also used in single-order, long-slit mode, with a  $0''.5$  slit, the *f/7* camera, and the grating in third order. The resulting dispersion was  $3.70 \text{ \AA pixel}^{-1}$ . We selected the grating angle to cover the spectral region from  $2.09$  to  $2.40 \mu\text{m}$ . For the CTIO run, the conditions were photometric, and the seeing was excellent (with an average FWHM near  $0''.5$ ). Unfortunately, the conditions at IRTF were not photometric on any of the six

<sup>3</sup> See <http://irtfweb.ifa.hawaii.edu/Facility/spex/>.

<sup>4</sup> For more on OSIRIS, go to [http://www.ctio.noao.edu/instruments/ir\\_instruments/osiris/index.html](http://www.ctio.noao.edu/instruments/ir_instruments/osiris/index.html).

nights, with the combined loss of two nights due to fog and clouds. The first of the observing runs at IRTF also had poor seeing (FWHM  $>1''.2$ ). The poor seeing at IRTF was partly due to the loss of the dome air-conditioning system. During the 2003 May IRTF run, however, the seeing was excellent, eventually reaching FWHM  $0''.4$  in the predawn hours.

The observing procedure was nearly identical for both observing runs. The spectra obtained with OSIRIS used a script that took five individual exposures along the slit, each separated from the preceding by  $8''$ . For just about all of the cataclysmic variables, the exposure times were 4 minutes in length. For the data obtained using SpeX, a similar observing routine was employed, but one in which data at six separate positions along the slit were obtained. Typical exposure times with SpeX were 3 minutes. For all of the program objects observed using OSIRIS, observations of nearby A stars were obtained just before, or after, the observational sequence for each target to correct for telluric features. For the SpeX runs, however, we switched to the use of early G dwarfs for the correction of telluric features as outlined by Maiolino, Rieke, & Rieke (1996). As a result of the longer observational sequences for the fainter sources, observations of telluric standards were often obtained in the middle of a sequence if the change in air mass was significant ( $\Delta AM > 0.1$ ). Finally, observations of a number of bright, late-type stars were obtained to act as spectral type templates. While the exposure times for these bright objects were quite short, the same scripts as used for the CV observations were employed.

To remove the sky background and dark current from each exposure with OSIRIS (SpeX), we subtracted the median of the other four (five) exposures obtained in that observing sequence. This process resulted in five (six) background-subtracted exposures from which the spectra were extracted using the normal IRAF methods. The spectra were wavelength-calibrated by extraction of an arc spectrum at the position (“aperture”) of each spectrum.

After wavelength calibration, groups of spectra for a CV were combined to form a single spectrum, and this was divided by the most appropriate telluric standard. If several of these divided spectra were created, as was the case for some of the fainter CVs, they were medianed together to form a final spectrum for the source. The OSIRIS spectra, having been divided by an A star, were then multiplied by a blackbody of the appropriate temperature and  $K$ -band flux to create “flux-calibrated” spectra. We caution against any interpretation of the profile of the  $H\ I\ Br\gamma$  line emission in the CV spectra obtained with OSIRIS. Because A dwarfs were used for telluric correction of the OSIRIS data, all of which have significant  $H\ I\ Br\gamma$  absorption, excess, false  $H\ I$  emission is produced upon division. We decided not to attempt to construct  $H\ I$ -free A stars for the final telluric division, because of the fact that we were uninterested in the  $H\ I$  emission.

The SpeX data were reduced in the same fashion, but instead of using A-type dwarfs, we observed early G-type dwarfs. The procedure for the use of G-type dwarfs to correct for the telluric features in near-infrared spectra has been described by Maiolino et al. (1996). G stars are useful for telluric correction because they have very few strong absorption lines in the near-infrared. But simple division of a program object’s spectrum by that of an early G-type dwarf does leave residual features due to  $H\ I$  absorption and weak metal lines in the G dwarf spectrum. Maiolino et al. have developed an IRAF

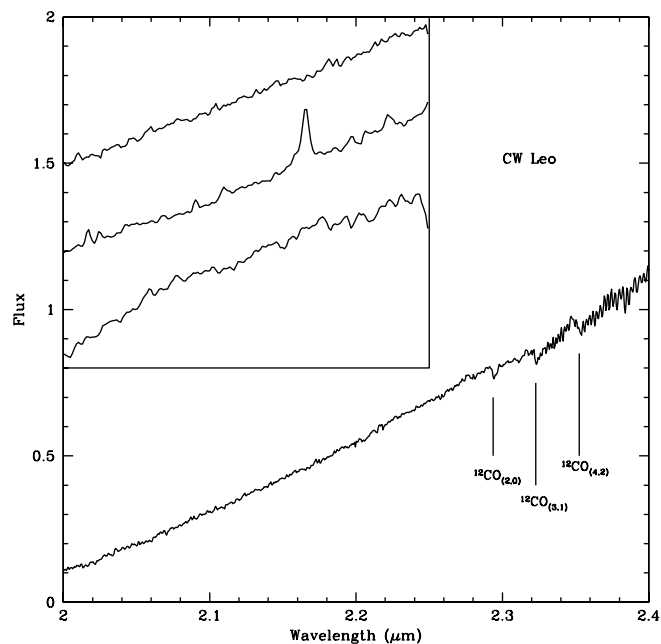


FIG. 1.—The  $K$ -band spectrum of proto-planetary nebula CW Leo (=IRC +10216). Shortward of  $2.29\ \mu\text{m}$ , the spectrum of CW Leo is free of strong absorption features. In the inset, we show an expanded view (the flux scale of the inset is twice that of the full spectrum) of the region spanning  $2.10$ – $2.20\ \mu\text{m}$ . In this inset, the bottom spectrum is the raw, extracted spectrum before division by the spectrum of a G dwarf star. The middle spectrum is after division by the G dwarf, revealing false emission lines due to weak absorption features in the G star spectrum (the strongest of these is  $H\ I\ Br\gamma$  at  $2.1655\ \mu\text{m}$ ). The final spectrum is constructed by the multiplication of a modified solar spectrum that has been smoothed to the resolution of the SpeX instrument and corrected for the radial velocity of the template star using an IRAF routine developed by Maiolino et al. (1996).

routine that modifies a high-resolution infrared spectrum of the Sun for the radial and rotational velocities of the telluric standard. It then smooths this spectrum to the resolution of the spectrograph used to observe the telluric standard. We followed their procedure to correct the data obtained using SpeX. Because some of the same spectral features are expected to be present in both the G star and CV secondary-star spectra, we felt that a test of how well such features are eliminated by this procedure was warranted. To perform this exercise, we observed the proto-planetary nebula CW Leo (IRC +10216), an object whose infrared spectrum is almost completely free of atomic or molecular absorption features (though weak absorption features of CO and other molecules can be seen longward of  $2.29\ \mu\text{m}$ ). The final  $K$ -band spectrum of CW Leo is presented in Figure 1. We have highlighted the region around  $H\ I\ Br\gamma$  in the inset to show how successfully the telluric absorption is removed, as are features introduced by the division of the G dwarf spectrum (such as an  $H\ I\ Br\gamma$  “emission” line). In the final, high-S/N spectrum, there are no residual features more than a few percent above or below the continuum.

The final, fully reduced (but unsmoothed) spectra obtained using SpeX (SY Cnc, RU Peg, CH UMa, TT Crt, AC Cnc, EM Cyg, V426 Oph, SS Cyg, and AH Her) are shown in Figures 2 and 3. The spectra obtained using OSIRIS (for V442 Cen, MU Cen, TT Crt, and BV Pup) are shown in Figure 4. Note that there remains some low-level fringing in the OSIRIS spectra, confined to the region between  $2.21$  and  $2.26\ \mu\text{m}$ , that we were unable to remove. We present the unsmoothed spectra in

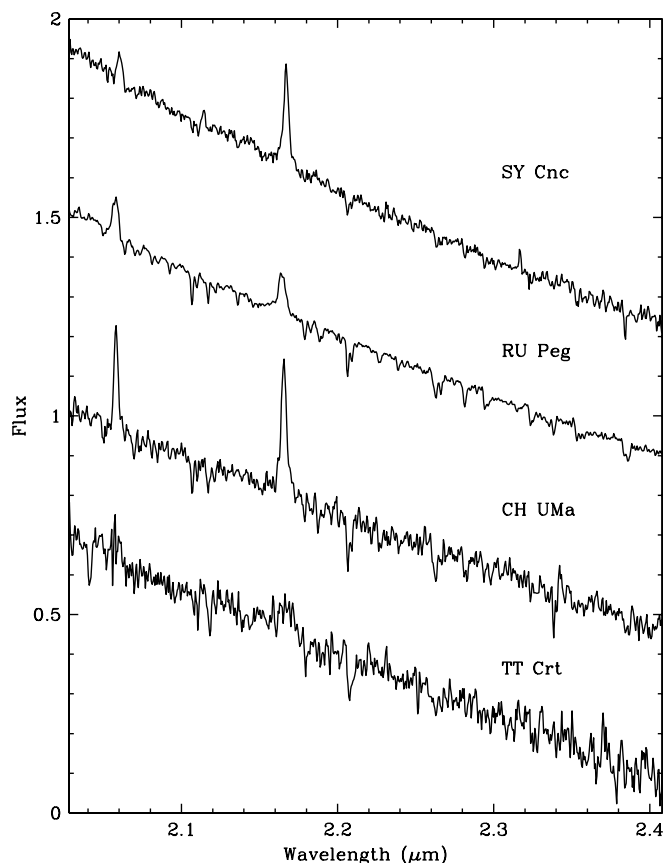


FIG. 2.—The final, but unsmoothed  $K$ -band spectra of SY Cnc, RU Peg, CH UMa, and TT Crt obtained using SpeX.

these figures so that the reader can determine for themselves the noise level, and the strength and/or reality of various features as ascertained from the smoothed spectra of the individual CVs to be discussed in the next section. A journal of our observations is presented in Table 1.

### 2.1. Accounting for Orbital “Smearing”

Because of the faintness of the program CVs, and the long observing sequences necessary to obtain useful data, the production of a final spectrum can be compromised by the orbital motion of the secondary: by simply medianing spectra from all of the data obtained for a particular object, the narrow features of the secondary star are smeared out. To properly account for this requires an ephemeris and radial velocity curve for the CV, and then a Doppler correction of each individual spectrum before the final result can be produced from their median. We have listed the orbital phase coverage for the program objects in Table 1. For those objects with accurate ephemerides, we list the run in orbital phase covered by our observations. For V442 Cen such ephemerides do not exist, and thus only the percentage of an orbital period covered by our observations is listed. Given an accurate ephemeris, it is rather easy to correct the spectra for the orbital motion, and this has been performed (when necessary) for each of the objects except V442 Cen.

## 3. THE $K$ -BAND SPECTRA OF CV SECONDARY STARS

Before we enter into a discussion of the individual spectra, we take a moment to address two issues that frequently arise that attempt to cast doubts on efforts to interpret the secondary-

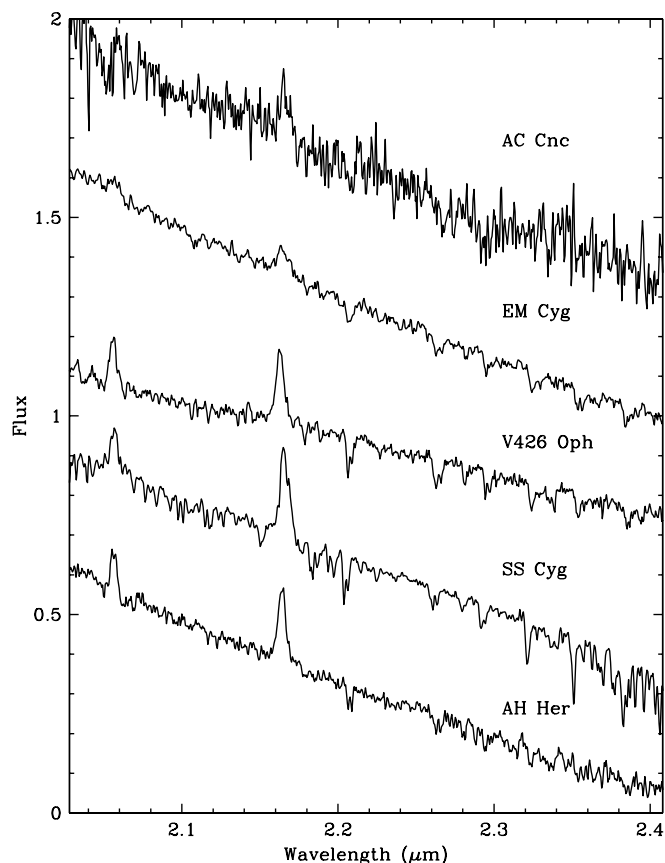


FIG. 3.—Same as Fig. 2, but for AC Cnc, EM Cyg, V426 Oph, SS Cyg, and AH Her.

star spectra observed for many CV systems. The first issue is a claim that what appears to be a relatively normal stellar photospheric spectrum has, in fact, been generated by the accretion disk in the CV system. The second issue is that the contamination of the secondary star’s spectrum by the light from accretion processes is so great that it fills in, or veils, the various absorption lines to the point where very little useful information about the true nature of the secondary star can be gleaned. For both issues, SS Cyg is probably the most useful example to examine, in that it has both a luminous secondary star and a luminous accretion disk, and it has been intensively studied. The first issue is the easier of the two to deal with and can be logically dismissed by examining the profiles of the detected absorption lines with respect to their apparent velocity broadening. High-resolution optical spectra of SS Cyg by Martínez-Pais et al. (1994) reveal an early K-type spectrum that appears to supply 55% of the  $R$ -band luminosity. The spectral energy distribution deconvolution by Harrison et al. (2000) found that a normal main-sequence K2 V star at the distance of SS Cyg would supply about 60% of the observed  $R$ -band flux. For SS Cyg, analysis of the absorption-line spectrum for rotational broadening gives values of  $V_{\text{rot}} \sin i = 87 \pm 4 \text{ km s}^{-1}$  (Martínez-Pais et al. 1994),  $99 \pm 8 \text{ km s}^{-1}$  (Echevarría et al. 1989), and  $90 \pm 10 \text{ km s}^{-1}$  (Friend et al. 1990). These values are consistent with the predicted secondary-star rotational velocity using the observed (and estimated parameters) for SS Cyg:  $85 \pm 8 \text{ km s}^{-1}$  (Echevarría et al. 1989). The average of the measured semiamplitudes of the radial velocity curve for the secondary star in SS Cyg is  $K_{\text{abs}} = 154 \pm 2 \text{ km s}^{-1}$ .

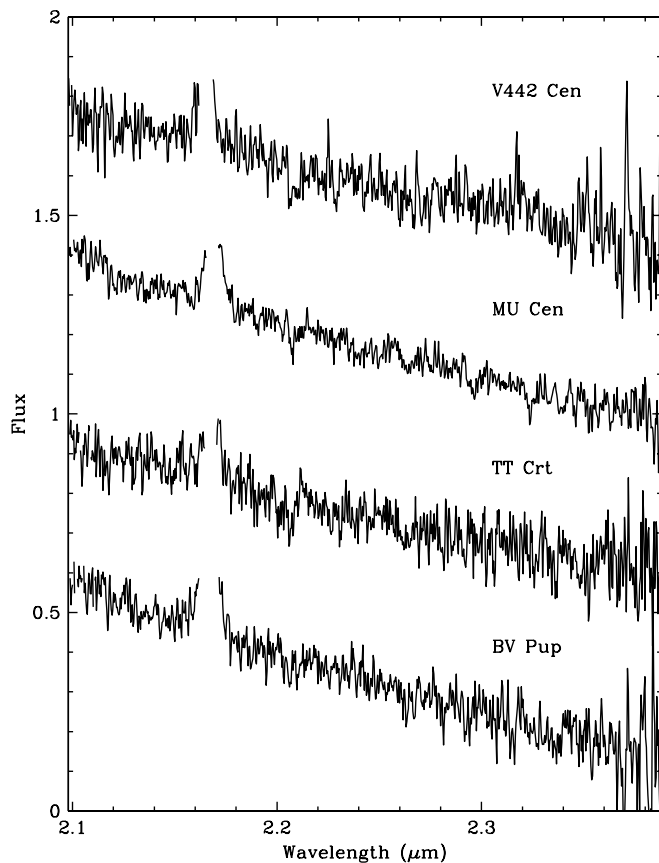


FIG. 4.—The final, unsmoothed OSIRIS spectra for V442 Cen, MU Cen, TT Crt, and BV Pup.

Obviously, if a late-type stellar spectrum were to be emitted from a point interior to the orbit of the secondary star, its velocity would have to be higher than that observed for the secondary star. It is also quite easy to surmise that if the entire accretion disk were engaged in producing the K dwarf spectrum, the resulting range in orbital velocities of the disk material would have dramatic consequences on the observed spectrum: the absorption lines should have *similar profiles* to the emission lines. For SS Cyg, the  $H\alpha$  profile is double peaked with a separation of  $526 \pm 14 \text{ km s}^{-1}$  between the peaks. Since the observed absorption lines are not doubled,

one must propose that the false stellar absorption spectrum is generated by a one-sided, narrow annulus in the accretion disk that somehow manages to both mimic a late-type stellar spectrum and produce more luminosity than the secondary star. If we choose this annulus to be on the outer edge of the disk (to keep its velocity broadening to a minimum) and let the disk extend to a radius that is 90% of the Roche L1 point in SS Cyg (50% of its semimajor axis), using equations from Warner (1995) we derive a Keplerian orbital velocity of  $V_{\text{orb}} = 344 \text{ km s}^{-1}$  for the material in this annulus (using  $i = 40^\circ$ , from Martínez-Pais et al. 1994), more than twice the observed value of  $K_2$ .

There is little doubt that the spectrum of the secondary star for some CVs is heavily contaminated by emission from other sources in the binary system. This is mostly evident through the deviation of the slope of the continuum from that of an uncontaminated late-type star. Some of the infrared spectra that we will discuss below appear to have continua that differ from that of an isolated late-type star. Since no models exist that have fully explained their quiescent spectral energy distributions, it is difficult to deconvolve the various contaminating components in a CV system to allow us to fully extract the underlying secondary-star spectrum. Our use of the highest available resolution has helped diminish the contamination of the narrow photospheric lines by the accretion disk (or white dwarf), as can be seen by comparing the  $R \approx 2000$  spectrum of SS Cyg shown in Figure 5 with the  $R \approx 1200$  spectrum shown in Figure 3 of Dhillon & Marsh (1995).

The real issue is how the contamination limits our ability to extract spectral types or other information from infrared spectra. For heavily contaminated sources, the contamination dramatically affects the spectrum and must be accounted for before we can determine the nature of the secondary star. For the long-period CVs presented in this paper, however, we find that the deviation from a pure, late-type stellar spectrum is generally quite minimal. Thus, it is rather simple to use the relative strengths of various absorption features to estimate the spectral type of the secondary star. Note that using the relative strengths of features located in close proximity to each other greatly reduces the effect of contamination, because the relative amount of contamination due to other sources does not change significantly over a small wavelength interval. For example, there are two spectral forms that are expected to be the main components of any contaminating sources in CVs: hot blackbody emission (from the white dwarf and/or hot

TABLE 1  
OBSERVATION JOURNAL

Object	Instrument	Date	Start (UT)	Stop (UT)	Phase
V442 Cen.....	OSIRIS	2002 Feb 21	0512	0628	11.5%
SY Cnc.....	SpeX	2003 May 19	0520	0623	0.64–0.75
RU Peg.....	SpeX	2003 May 18	1439	1508	0.63–0.68
CH UMa .....	SpeX	2003 May 17	0712	0747	0.53–0.60
MU Cen .....	OSIRIS	2002 Feb 22	0751	0840	0.03–0.13
TT Crt .....	OSIRIS	2002 Feb 22	0612	0716	0.36–0.51
	SpeX	2003 May 17	0808	0934	0.24–0.43
AC Cnc .....	SpeX	2003 May 18	0522	0654	0.64–0.75
EM Cyg.....	SpeX	2003 May 18	1221	1305	0.08–0.19
V426 Oph .....	SpeX	2003 May 17	0958	1012	0.26–0.31
SS Cyg.....	SpeX	2002 Apr 7	1505	1546	0.74–0.84
BV Pup .....	OSIRIS	2002 Feb 21	0340	0425	0.97–0.08
AH Her .....	SpeX	2003 May 18	0827	0907	0.14–0.24

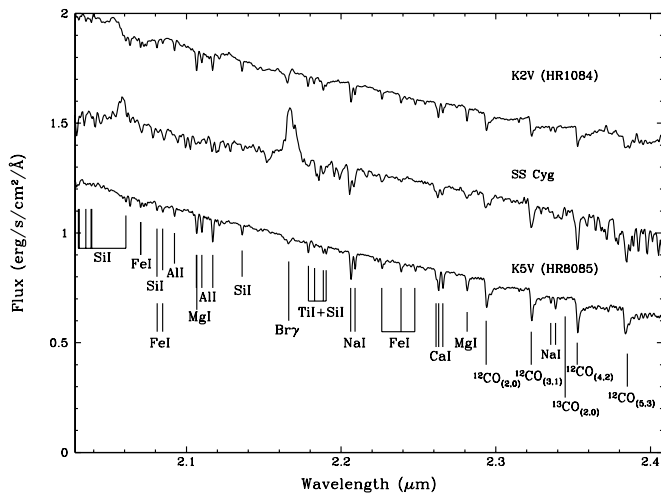


FIG. 5.—The (unsmoothed)  $K$ -band spectrum of SS Cyg. We compare the SS Cyg spectrum with that of K2 V and K5 V templates from Wallace & Hinkle (1997). We identify the most prominent atomic and molecular absorption features below the spectrum of the K5 V template.

spot) and some type of power-law source (from the accretion disk). Combinations of both of these, or even several different such components, are probably the most likely contaminating sources. But to strongly affect two closely spaced absorption lines requires a contaminating continuum source that changes dramatically over a short wavelength range. Of the various possible contaminants, a pure blackbody will impart the greatest change, because of fact that its  $F_{\lambda} \propto \lambda^{-4}$  dependence is much steeper than either the expected steady state accretion disk spectrum, where  $F_{\lambda} \propto \lambda^{-7/3}$ , or the spectrum of free-free emission ( $F_{\lambda} \propto \lambda^{-2}$ ). For a 20,000 K blackbody in the  $K$  band, twice as much flux is emitted at 2.00  $\mu\text{m}$  versus 2.40  $\mu\text{m}$ . But when comparing two nearby features, such as the Na I doublet (centered near 2.207  $\mu\text{m}$ ) and the Ca I triplet (centered near 2.263  $\mu\text{m}$ ), the difference is only 3%! Thus, even in situations where the overall contamination level is high, the *relative* contamination between closely spaced absorption features is negligible. As long as limited spectral ranges are used when comparing spectral features, their relative strengths will be valid indicators of the true nature of the underlying spectrum. This is the process we will use below to estimate spectral types, as well as to make statements about apparent abundance enhancements or deficits.

In what follows, we describe the  $K$ -band spectra for each individual object. In most cases, the spectra presented in Figures 2, 3, and 4 have been smoothed to improve their S/N. We will compare the smoothed CV spectra with those of identically smoothed spectral templates that we have obtained using OSIRIS or SpeX, or with those from the catalog of  $K$ -band spectra for normal stars by Wallace & Hinkle (1997). In our spectral analysis, we have used  $K$ -band line identifications from Wallace et al. (1996) and from Hinkle, Wallace, & Livingston (1995). For each of the CVs, we have rotationally broadened the spectral type templates to match the observed, or predicted, rotational broadening of the secondary star. We order the following discussion by orbital period from the longest to shortest.

### 3.1. V442 Centauri

In the Ritter & Kolb (1998) catalog, the orbital period of V442 Cen is listed as  $P_{\text{orb}} = 11.0$  hr. In the Downes et al.

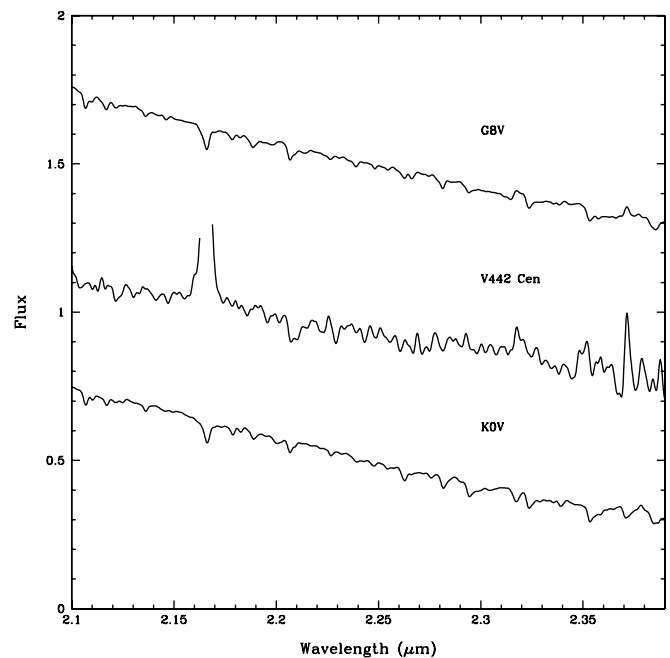


FIG. 6.—Spectrum of V442 Cen compared with those of a G8 V and K0 V. All three spectra have been smoothed to a FWHM resolution of 40 Å using the GAUSS routine in IRAF.

(2001) Catalogue and Atlas of Cataclysmic Variables, however, there is some doubt cast on the reliability of this period. Warner (1995, p. 109) shows that systems with such long periods probably have to have evolved secondaries in order to fill their Roche lobes. The  $K$ -band spectrum of V442 Cen obtained with OSIRIS, shown in Figure 6, is the median of fifteen 4 minute exposures. At first glance, the spectrum is unusual compared with the other objects in our sample in that it lacks strong absorption features, and redward of 2.3  $\mu\text{m}$  the spectrum is choppy. While the Na I doublet is strong, suggesting a late-type star, there appears to be little evidence for  $^{12}\text{CO}$  absorption. The key to deriving a spectral type is the hump at 2.317  $\mu\text{m}$ . This feature is an “opacity minimum” that shows up in mid- to late-type G dwarfs. It arises because in the earlier G-type dwarfs, a strong pair of iron lines are present that absorb the blue half of this hump. In later G dwarfs, the  $^{12}\text{CO}$  (3–1) transition comes into play and whittles away at the hump from the red side. This is shown in Figure 7, where we have compared the red end of the  $K$ -band spectrum of V442 Cen with those of a G3 V and a G8 V star. The hump from the opacity minimum appears to be stronger in V442 Cen than for any normal main-sequence dwarf, suggesting weaker iron or  $^{12}\text{CO}$  absorption than normal. Note that this feature does not show up in G giants and subgiants, because of their much stronger  $^{12}\text{CO}$  absorption. There is another opacity minimum at 2.372  $\mu\text{m}$ , caused by a gap in the CO absorption, which appears to be even stronger in V442 Cen. However, the S/N in this region is quite low and is probably partly responsible for its large observed amplitude. We assign a spectral type of  $G6 \pm 2$  for the secondary star. After typing the secondary star, examination of the spectrum reveals that the expected atomic absorption features are present at their normal levels with, perhaps, slight enhancements in Na and Mg. As shown in Figure 6, the continuum of V442 Cen is substantially redder than a G8 V and is even redder than a K0 V. Given these peculiar features,

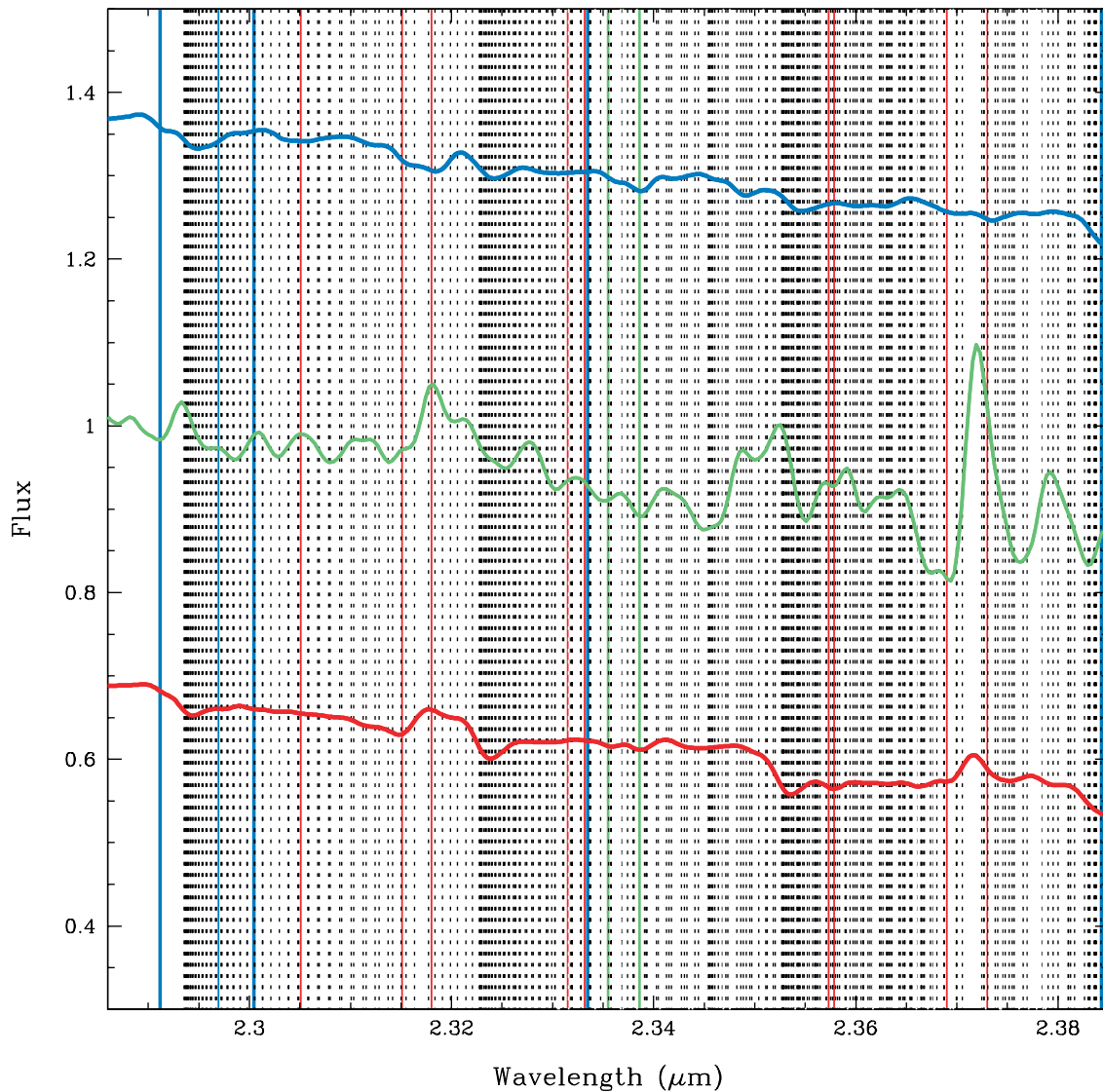


FIG. 7.—Close-up of the red region of the V442 Cen spectrum (*green*), showing the location of the two opacity minima described in the text. Also plotted are the *K*-band spectra of G3 V (*blue*) and G8 V (*red*) templates. In this figure, the individual lines from the vibrational/rotational transitions of the CO molecule are plotted as vertical dotted lines, Fe I lines are indicated in red, and green lines are Na I, while blue lines are Ti I. In the hotter (G2 V) star, the Fe I lines absorb the continuum at  $2.317 \mu\text{m}$ ; in later-type stars (>G8 V), the  $^{12}\text{CO}$  (3–1) band head becomes stronger and completely removes this feature. The strength of the opacity minimum in V442 Cen is greater than any normal G dwarf, suggesting a deficit of iron, CO, or both, though neither of these species appears to be underabundant.

additional high-S/N observations of V442 Cen are clearly warranted.

### 3.2. *SY Cancri*

SY Cnc has an orbital period of 9.120 hr and has been classified as a member of the *Z Camelopardalis* family of cataclysmic variables. Vande Putte et al. (2003) have used the technique of skew mapping to extract an updated ephemeris for the system, a radial velocity curve, a derived mass ratio of  $q = M_2/M_1 = 0.68$ , and a primary mass of  $M_1 = 1.54 \pm 0.40 M_\odot$ . These values suggest a secondary star with a mass near  $1.0 M_\odot$ . From these parameters, we estimate a very low rotational broadening of  $V_{\text{rot}} \sin i = 45 \text{ km s}^{-1}$ . Our data set consists of eighteen 3 minute exposures with SpeX, and the final smoothed spectrum is shown in Figure 8. The American Association of Variable Star Observers (AAVSO) light-curve database indicates that SY Cnc was in outburst, with  $m_v \approx 11.5$ , at the time of our observations.

The spectrum of SY Cnc is consistent with that of an early G-type star. Careful comparison of SY Cnc with the G1.5 V (HR 7503) and G3 V (HR 7504) templates indicates a slightly better match to the G1.5 V. This would be consistent with the secondary star's mass noted above. In addition to the He I line at  $2.058 \mu\text{m}$ , the He I triplet at  $2.112 \mu\text{m}$  is also in emission. Except for Si I, which appears to be somewhat underabundant, all of the absorption features appear to be at the proper strength for an early G-type dwarf. The peak due to the opacity minimum at  $2.317 \mu\text{m}$  is stronger in SY Cnc than in either of the templates, suggesting somewhat weaker Fe I absorption, though none of the other prominent iron lines seem to be significantly weaker than those of the templates. The final feature of interest is the slope of the continuum: in its outburst state, the slope of the *K*-band continuum in SY Cnc is redder than the G star templates, implying that the outburst accretion disk has a significantly flatter spectral slope than a 6000 K blackbody.

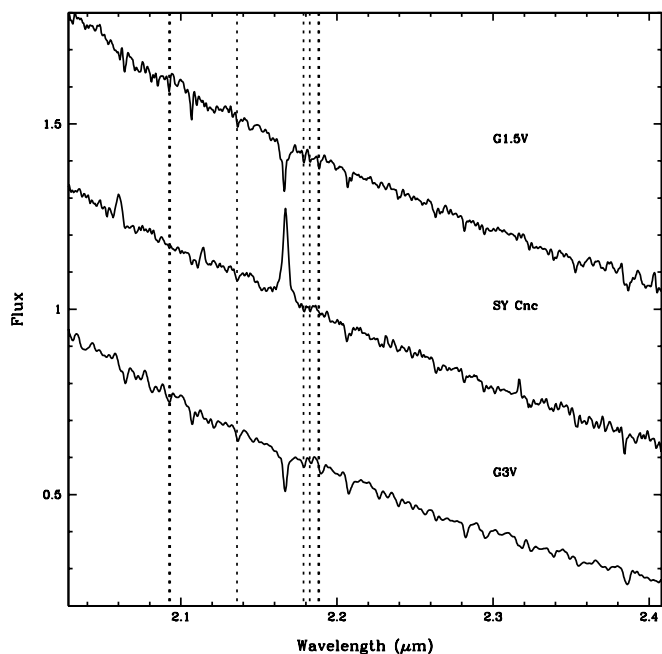


FIG. 8.—Spectrum of SY Cnc (smoothed to  $\text{FWHM} = 20 \text{ \AA}$ ) compared with the spectra of a G1.5 V and a G3 V template. SY Cnc also shows an apparent emission feature at  $2.317 \mu\text{m}$  due to the opacity minimum described for V442 Cen in Fig. 7. The dotted vertical lines in this plot denote the locations of the strongest Si I lines in the  $K$ -band spectra of cool stars. It is clear that the Si I features in the spectrum of SY Cnc are weaker than those of the template dwarfs.

### 3.3. RU Pegasi

RU Peg has an orbital period of 8.990 hr and, with  $K_{2\text{MASS}} = 10.46$ , is one of the brightest CVs in the infrared. The unsmoothed SpeX spectrum of RU Peg, shown in Figure 9, is the median of twelve 2 minute exposures and covers only 0.05 in orbital phase. Friend et al. (1990) derived the following

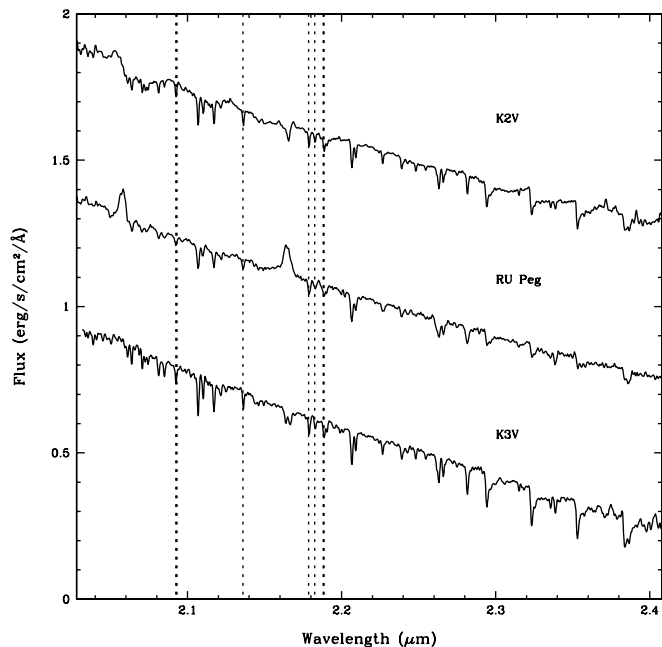


FIG. 9.—Unsmoothed spectrum of RU Peg compared with K2 V and K3 V templates. As in Fig. 8, the dotted vertical lines are the locations of the Si I lines.

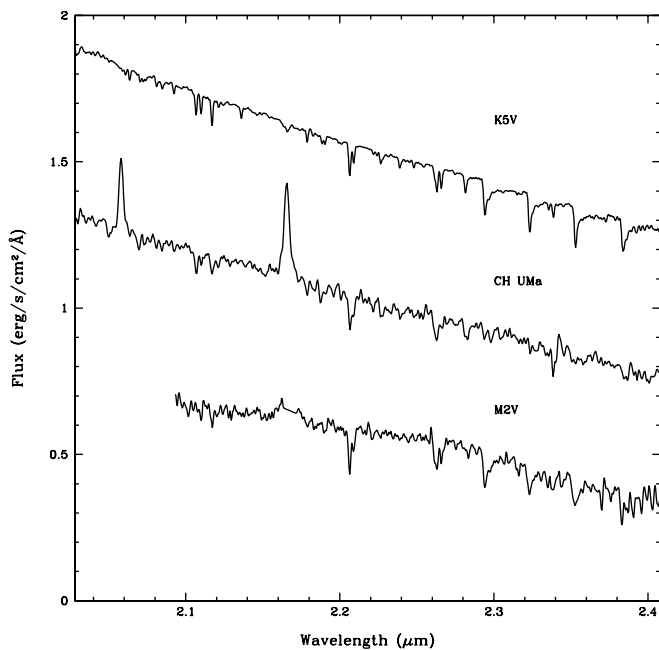


FIG. 10.—Smoothed ( $\text{FWHM} = 20 \text{ \AA}$ ) spectrum of CH UMa compared with the spectrum of a K5 V template from Wallace & Hinkle (1997) and that of an M2 V (GJ 393) obtained using OSIRIS (the region around H I Br $\gamma$  at  $2.1655 \mu\text{m}$  has been patched over).

systemic parameters:  $K_2 = 121 \text{ km s}^{-1}$ ,  $V_{\text{rot}} \sin i = 80 \text{ km s}^{-1}$ ,  $M_2 = 1.07 \pm 0.02 M_{\odot}$ , and a spectral type of K3. Friend et al. note that the spectral type and mass are not consistent, and they suggest that the secondary star in RU Peg probably has begun to evolve off of the main sequence (see § 4.2). Comparison of RU Peg with the spectra of early K dwarfs indicates a best-fit spectral type of K2. Analysis of the strengths of the absorption lines indicates only two anomalies: weak Si I and CO. The strongest absorption features from both Si and CO appear to be about one-half the strength they should be for a spectral type of K2. These deficits appear to be confirmed from the preliminary analysis of a *FUSE* spectrum of RU Peg by Sion et al. (2002), which indicates that the white dwarf in RU Peg is underabundant in both carbon (0.1 times solar) and silicon (0.1 times solar).

### 3.4. CH Ursae Majoris

As in the case of RU Peg, Friend et al. (1990) find a cooler than expected spectral type (M0) for the secondary star in CH UMa. For an orbital period of 8.232 hr, and assuming a main-sequence mass-radius relationship, a G-type star would have been predicted. An analysis of archival *IUE* spectra of CH UMa by Dulude & Sion (2002) reveals a large N v/C iv ratio, similar to those described by Gänsicke et al. (2003), suggesting an enhanced level of nitrogen and a deficit of carbon. Our spectrum of CH UMa, which consists of twelve 3 minute exposures, is presented in Figure 10. Friend et al. estimate that  $V_{\text{rot}} \sin i \leq 45 \text{ km s}^{-1}$ , and we have chosen to broaden our template spectra by  $40 \text{ km s}^{-1}$ . The spectral type of the secondary star and the  $K$ -band continuum are consistent with a  $K7 \pm 2$ , except for the extremely weak CO features. A number of other features may be unusual [such Ti I at  $2.28 \mu\text{m}$ , and  $^{13}\text{CO} (2-0)$ ], but they await spectra with higher S/N. The relatively narrow, single-peaked H I and He I emission lines are consistent with the low orbital inclination angle of  $i = 21^\circ \pm 4^\circ$  found by Friend et al. (1990).

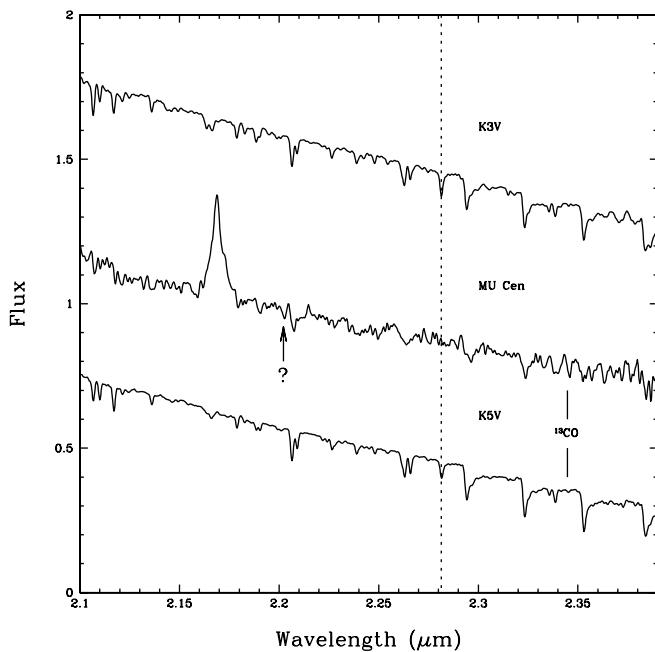


FIG. 11.—Spectrum of MU Cen compared with those of K3 V and K5 V templates. The location of the  $^{13}\text{CO}$  band head is marked. All three spectra have been smoothed to  $\text{FWHM} = 20 \text{ \AA}$ . The vertical dotted line is the location of the  $2.281 \mu\text{m}$  Mg I line, which appears to be extremely weak in the spectrum of MU Cen. The arrow points to the location of an unidentified absorption feature (at  $2.201 \mu\text{m}$ ) seen in the spectra of several of our program objects.

### 3.5. MU Centauri

MU Cen is a well-known CV having a radial velocity curve for the secondary (Friend et al. 1990) from which an orbital period ( $8.208 \text{ hr}$ ), mass ratio ( $q = 0.83 \pm 0.15$ ), and secondary-star rotational velocity ( $V_{\text{rot}} \sin i = 110 \pm 15 \text{ km s}^{-1}$ ) have been derived. We used the observed value for  $V_{\text{rot}} \sin i$  to broaden the template spectra for comparison with the spectrum of MU Cen presented in Figure 11. This spectrum was constructed from data obtained with OSIRIS and is the median of ten 4 minute exposures. Ten percent of an orbital period was covered by our observations. The continuum slope of MU Cen is identical to mid K-type stars, suggesting little if any contamination. The Na I doublet and the Ca I triplet have peculiar profiles but have roughly the correct depth for a spectral type near K5. We assign a spectral type of  $\text{K}4 \pm 1$ . This spectral type is consistent with the results of Friend et al. (1990), which indicated a spectral type earlier than K7 V. However, the  $^{12}\text{CO}$  features and the Mg I line (at  $2.2814 \mu\text{m}$ ) are too weak for a mid K-type star. In addition, both silicon and iron seem to be slightly enhanced. To the blue side of the Na I doublet, at  $2.201 \mu\text{m}$ , is an absorption feature that appears in many of our CV spectra (it is seen in the spectrum for V442 Cen, for example), but one whose origin is not obvious. There is a Ti I line near this position ( $2.2010 \mu\text{m}$ ), but this would require a much greater enhancement than is indicated by the other Ti I lines. The most striking feature in the spectrum of MU Cen is the strong  $^{13}\text{CO}$  (2–0) band head at  $2.345 \mu\text{m}$ . A check on the reality of this feature can be made by putting it in context with the sequence of features running from  $^{12}\text{CO}$  (3–1) ( $2.321 \mu\text{m}$ ) to the red Na I doublet ( $2.336 \mu\text{m}$ ) and  $^{12}\text{CO}$  (4–2) ( $2.354 \mu\text{m}$ ). Given the local S/N in this region, it is obvious that the strength of this feature could differ by  $\pm 20\%$ , but this would still indicate an extreme enhancement of

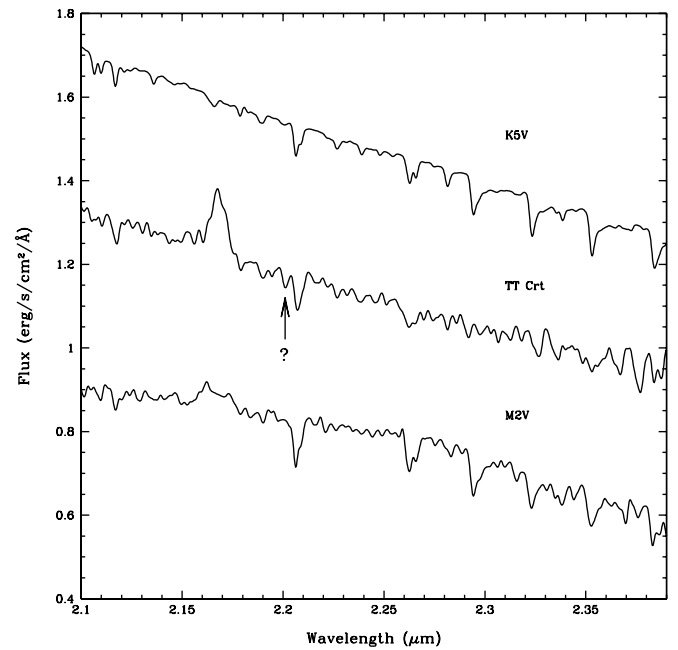


FIG. 12.—Spectrum of TT Crt. This spectrum is the mean of data sets from both OSIRIS and SpeX and has been smoothed to  $\text{FWHM} = 40 \text{ \AA}$  and compared with identically smoothed K5 V and M2 V spectral type templates. As in Fig. 11, the location of an unidentified line at  $2.201 \mu\text{m}$  is indicated with an arrow.

$^{13}\text{CO}$ . Comparison of the MU Cen spectrum with those of red giants with strong  $^{13}\text{C}$  enhancements indicates a  $^{12}\text{C}/^{13}\text{C}$  ratio close to that of “CNO completion.”

### 3.6. TT Crateris

TT Crt is a long-period ( $7.3 \text{ hr}$ ), high-inclination ( $i > 50^\circ$ ) dwarf nova studied by Szkody et al. (1992). We have used their value of  $q = 0.8$  to estimate a rotational velocity for the secondary star of  $V_{\text{rot}} \sin i = 109 \text{ km s}^{-1}$  and have applied this amount of broadening to the template star spectra. TT Crt was observed using both OSIRIS and SpeX. A single spectrum was produced from the OSIRIS data that is the median of fifteen 4 minute exposures, and this was combined with the SpeX spectrum of TT Crt, which is the median of twenty-four 3 minute exposures. TT Crt is faint ( $K_{2\text{MASS}} = 13.19$ ), and the smoothed spectrum presented in Figure 12 is the mean of the OSIRIS and SpeX data sets. Comparison of the Na I, Ca I, and Mg I (at  $2.281 \mu\text{m}$ ) absorption features gives a best-fitting spectral type of K5 V, consistent with the results of Szkody et al. (1992), though the Ca I triplet is somewhat too weak for this spectral type. There is almost no evidence of  $^{12}\text{CO}$  absorption! As in the spectra for V442 Cen and MU Cen, the absorption feature at  $2.201 \mu\text{m}$  is quite strong. While our final spectrum of TT Crt is rather poor, absorption lines from Ti I, Si I, and Fe I appear to be at their normal strengths, while those of Al I might be slightly enhanced.

### 3.7. AC Cancri

AC Cnc is a rarely observed eclipsing, nova-like variable that has an orbital period of  $7.211 \text{ hr}$  and  $K_{2\text{MASS}} = 12.59$ . Optical observations indicate a late G or early K spectral type for the secondary star and a mass ratio of  $q = 1.24 \pm 0.14$  (Schlegel, Kaitchuck, & Honeycutt 1984). The spectrum presented in Figure 13, which consists of eighteen 3 minute exposures, is very poor as a result of the presence of patchy

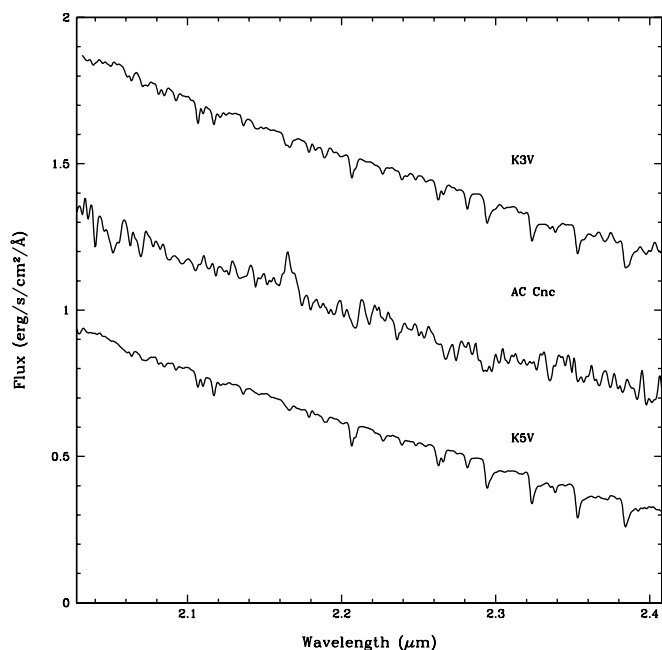


FIG. 13.—Spectrum of AC Cnc compared with K3 V and K5 V templates. The three spectra have been smoothed to FWHM = 40 Å.

clouds. Assuming a normal level of CO absorption, the spectral type of the secondary appears to be somewhat later than K5. The continuum, however, appears to be redder than this, and the spectral type could be as late as M2 if the CO features are weaker than normal. Given its long orbital period, a dynamically unstable value for its mass ratio ( $q > 1$ ), and the suggestion of a fairly late spectral type, AC Cnc certainly warrants additional attention.

### 3.8. EM Cygni

EM Cyg is a bright ( $K_{2\text{MASS}} = 11.15$ ), well-known Z Camelopardalis type dwarf nova with an orbital period of 6.982 hr, and it has a secondary star with a spectral type of K2–K5. Recently, North et al. (2000) have found that the light from the system is contaminated by a third star, possibly associated with EM Cyg, that is nearly identical in brightness and temperature to the secondary. With this discovery, North et al. were able to derive a revised value for the mass ratio of  $q = 0.88 \pm 0.05$ , down from the dynamically unstable value of  $q = 1.26$  found by Stover, Robinson, & Nather (1981). The *K*-band spectrum of EM Cyg is shown in Figure 14 and consists of twelve 3 minute exposures. North et al. (2000) found a rotational broadening of  $140 \pm 6 \text{ km s}^{-1}$  for the secondary star in EM Cyg, and we have broadened the template spectra by this amount.

The spectrum of EM Cyg is actually surprisingly peculiar. Comparison of all of the main molecular and atomic absorption features indicates a spectral type that is slightly earlier than K0. For example, the Mg I and Al I lines near  $2.11 \mu\text{m}$ , the sodium doublets, and the CO features are slightly weaker in strength than those of a K0 V template, while the Ca I triplet in EM Cyg is stronger than that of a K0 V. The continuum, however, is much redder than a K0 V and is almost identical to that of our K5 V template. What seems most apparent is that all of the spectral features seem to be broader than those in the templates. We believe this is partly due to our radial velocity correction for the secondary star. Given that the third star

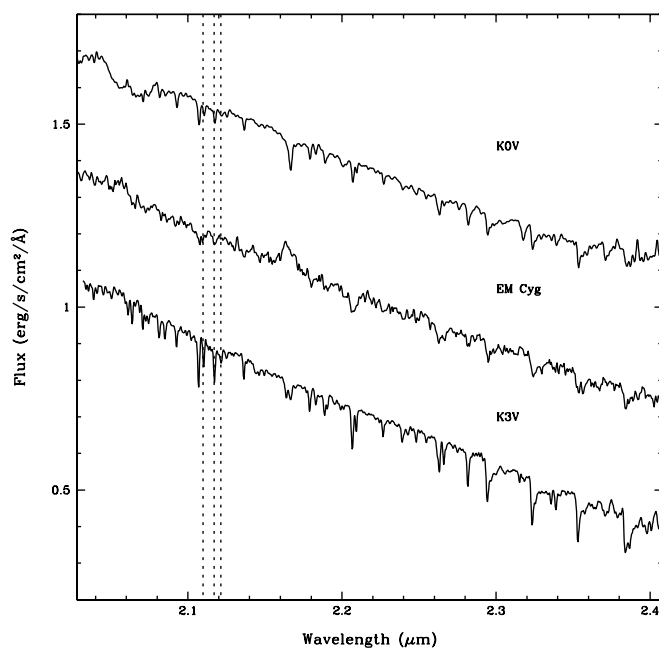


FIG. 14.—The (unsmoothed) spectrum of EM Cyg compared with those of K0 V and K3 V templates. The vertical dotted lines indicate the locations of the strongest Al I lines in the *K*-band spectra of cool dwarfs.

in the system is not moving, its spectral features would have been blueshifted by  $\sim 155 \text{ km s}^{-1}$  due to our correction for the velocity of the actual secondary star. We have tested this scenario assuming both stars have identical luminosities, and we find that the spectral features are indeed broader, but not as broad as those observed here. If we assume an early- or mid-type K star, then the lines of Al I and Ti I are weaker than they should be, even given the excess broadening of the absorption features. Another clearly detected anomaly is  $^{13}\text{CO}$ , which is several times stronger in the spectrum of EM Cyg than in the K3 V template.

### 3.9. V426 Ophiuchi

V426 Oph is a bright ( $K_{2\text{MASS}} = 10.33$ ) Z Camelopardalis CV with an orbital period of 6.848 hr. During outburst, V426 Oph reaches  $m_V = 10.9$  (Warner 1995, p. 130). During its standstills, it hovers near  $m_V = 11.9$ . Inspection of the AAVSO light-curve database indicates V426 Oph had  $m_V \approx 12.2$  at the time of our observations. Hessman (1988) has used time-resolved optical spectroscopy of V426 Oph to derive the orbital period, an updated ephemeris, a mass ratio ( $q = 0.78 \pm 0.06$ ), an orbital inclination ( $59^\circ \pm 6^\circ$ ), a secondary-star spectral type (K3), and primary and secondary masses (0.9 and  $0.7 M_\odot$ , respectively). We have used this solution to predict a value for the secondary star's rotational velocity of  $V_{\text{rot}} \sin i = 116 \text{ km s}^{-1}$ . The unsmoothed spectrum presented in Figure 15 is the median of six 2 minute exposures. Because of the brief time interval spent observing V426 Oph (0.03 in orbital phase,  $\Delta K_2 = 9 \text{ km s}^{-1}$ ), no radial velocity correction has been applied to its spectrum.

The slope of the continuum of V426 Oph is much flatter (redder) than those of early and mid K dwarfs, being similar to that of an M2 V, except for the lack of a decline due to water vapor absorption at the red end of the *K* band. The absorption features also show a mixture of strengths that span these two spectral classifications. For example, the Al I and Mg I lines near  $2.11 \mu\text{m}$  are quite weak, suggesting an early

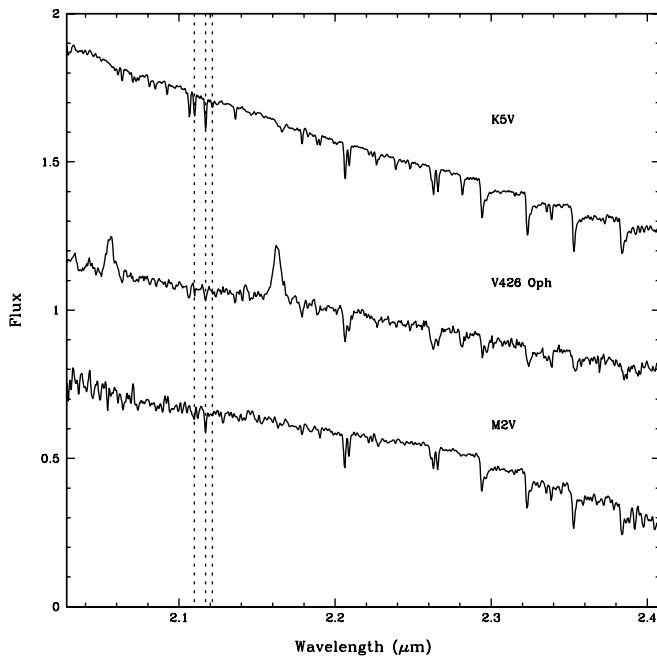


FIG. 15.—Unsmoothed spectrum of V426 Oph compared with K5 V and M2 V templates. The slope of the continuum in V426 Oph is the flattest of any of the 12 CVs presented in this paper. As in Fig. 14, the dotted vertical lines mark the locations of the strongest Al I lines.

M spectral type. The Na I doublet, Ca I triplet, and Mg I (at 2.281  $\mu\text{m}$ ) features have strengths similar to those of the K5 V template. The CO features are much too weak for any spectral type later than  $\approx$ K2 V. Given our results for SY Cnc, and because V426 Oph was 1.2 mag above minimum light, it seems likely that accretion disk contamination is causing the redder than expected spectral slope in V426 Oph. This allows us to reconcile our result with the K3 classification of Hessman (1988). By assigning a spectral type of K5 to the secondary in V426 Oph, we can then compare the relative strengths of various features. It is clear that the Al I lines and CO features are much weaker in the spectrum of V426 Oph than they should be if the secondary is a normal K dwarf, with both about half as strong as normal. All of the other atomic species (Si I, Ti I, Mg I, and Fe I) seem to be present at near-normal strengths.

### 3.10. SS Cygni

SS Cyg has an orbital period of 6.603 hr and, as discussed earlier, has  $V_{\text{rot}} \sin i = 87 \pm 4 \text{ km s}^{-1}$  (Martínez-Pais et al. 1994). We have applied this amount of rotational broadening to our template spectra. Because of SS Cyg's brightness, its spectrum (presented above in Fig. 5) is of very high quality, and it is composed of six 3 minute exposures. We have identified many of the strongest atomic and molecular lines for the K5 V template shown in Figure 5. Using the ephemeris of Martínez-Pais et al. (1994), the mean orbital phase at the time of our observations was 0.1, just past inferior conjunction of the secondary star. At first blush, the spectrum of SS Cyg appears to be that of a early-to-mid K-type dwarf. But closer examination reveals several peculiarities. For example, the strengths of the Ca I triplet and the first-overtone feature of  $^{12}\text{CO}$  closely resemble those of a K2 V. The Na I doublet, and the higher overtones of CO, however, are much closer in strength to those of a K5 V. Throughout the spectrum, the lines

of Mg I are very weak. Perhaps the most unusual region in the spectrum of SS Cyg is that between 2.08 and 2.13  $\mu\text{m}$ . The three Al I features (at 2.092, 2.110, and 2.117  $\mu\text{m}$ ) are not at their proper strengths, with the 2.110  $\mu\text{m}$  line being invisible. Between the 2.092 Al I line and the 2.106 Mg I line, there appears to be a doublet in the spectrum SS Cyg. The bluer member of this pair can be associated with an Fe I line, and its strength is roughly consistent with other nearby Fe I lines—but the strength of those lines would require excess iron absorption. A comparison of the strength of the Fe I features in the spectrum of SS Cyg between 2.20 and 2.30  $\mu\text{m}$  shows that iron does not appear to be overabundant. A possible origin for the red line of this doublet, and a number of other weak features in this region, including some of the overly strong Fe I lines, can be traced to the assignment of the isolated absorption feature at 2.127  $\mu\text{m}$  to CN. CN lines can then match the red line of the unidentified doublet, as well as previously unidentified absorption features at 2.077 and 2.085  $\mu\text{m}$ . As shown by the templates, CN absorption is not expected to be significant in early and mid K-type dwarfs.

Two other features of the SS Cyg spectrum deserve mention. The first is the presence of a weak  $^{13}\text{CO}$  (2–0) feature. While much weaker than that seen in MU Cen, the S/N of the SS Cyg spectrum is much higher, and this feature is certainly real. The other interesting aspect of the spectrum of SS Cyg is the overall slope of the continuum. The continuum of SS Cyg is flatter than those of mid-K dwarfs, and like SY Cnc and V426 Oph, there must be a significant flat-spectrum or additional red source contaminating the K-band spectrum.

Given all of these peculiarities, it is difficult to assign a unique spectral type to the secondary star of SS Cyg. We propose a spectral type of  $\text{K}4 \pm 2$  for the secondary star in SS Cyg. This spectral type should be compared with previous estimates of K4 (Harrison et al. 2000), K2 V (Echevarría et al. 1989), K2/K3 (Martínez-Pais et al. 1994), and K5 V (Friend et al. 1990).

### 3.11. BV Puppis

BV Pup is a dwarf nova that has an orbital period of 6.353 hr and exhibits low-amplitude outbursts. Modeling the infrared ellipsoidal variations of BV Pup, Szkody & Feiswog (1988) derived a high inclination of  $78^\circ \leq i \leq 90^\circ$  for the system and derived a mass of  $0.62 M_{\odot}$  for the secondary star. This contrasts with the analysis by Bianchini et al. (2001), who derive a much lower inclination of  $23^\circ \pm 3^\circ$  from a combination of spectroscopic observations and dynamical arguments. Bianchini et al. derive a much higher secondary-star mass of  $0.96 M_{\odot}$ , and a mass ratio of  $q = 0.80$ . They could not detect any evidence of features from the secondary star in their optical spectrum of this system. We used those results to estimate a rotational velocity broadening of  $61 \text{ km s}^{-1}$  for the BV Pup secondary. We observed BV Pup using OSIRIS, and the final spectrum, consisting of ten 4 minute exposures, is presented in Figure 16.

The spectrum for BV Pup has rather low S/N. The slope of the continuum suggests an early-to-mid K dwarf. Comparison of the relative strengths of the Na I and Ca I features indicates a spectral type near K3, as do the  $^{12}\text{CO}$  features. A normal, main-sequence K3 V should have a mass near  $0.72 M_{\odot}$ , suggesting the higher inclination model for BV Pup might be more appropriate. A higher inclination angle implies a larger rotational velocity, and this also seems to be consistent with the widths of the absorption features in the spectrum of BV Pup, which are broader than those of the modified template

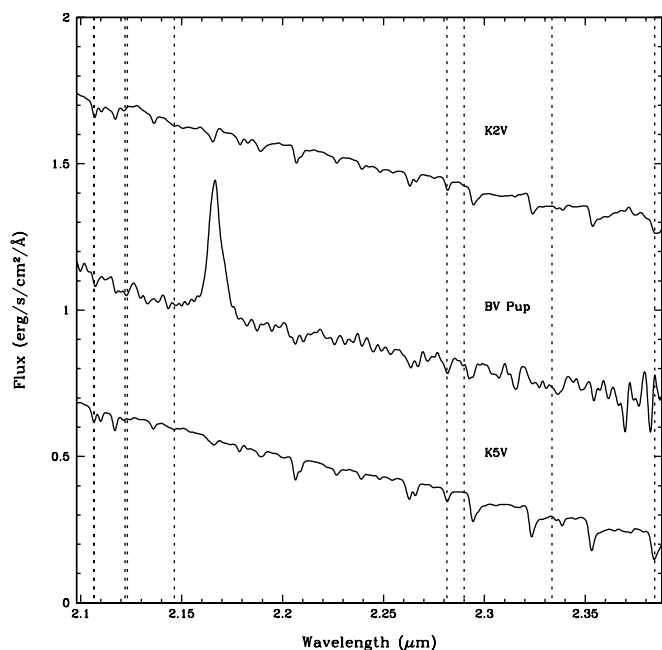


FIG. 16.—Smoothed (FWHM = 40 Å) spectrum of BV Pup compared with identically processed K2 V and K5 V templates. Like the other *K*-band spectra obtained using OSIRIS, the H  $\gamma$  Br $\gamma$  emission line at 2.1655  $\mu$ m is artificially enhanced because of the division of an A-type dwarf. The vertical dotted lines in this plot are the locations of the strongest Mg I lines in the spectra of late-type dwarfs. The strength of these lines seem to be slightly enhanced in the spectrum of BV Pup.

stars. The spectrum is too poor for an abundance analysis, though several lines of Mg I seem stronger than those of the K3 V template.

### 3.12. AH Herculis

AH Her is a Z Camelopardalis system with an orbital period of 6.195 hr that varies between a quiescent state where  $m_v = 14.3$ , a standstill level near  $m_v = 12.0$ , and outburst at  $m_v = 11.3$  (Warner 1995, p. 130). The AAVSO light-curve database indicates that AH Her was at  $m_v \approx 12.5$  at the time of our SpeX observations and on its way to a short-lived outburst that peaked about 2 days later at  $m_v = 11.5$ . Horne, Wade, & Szkody (1986) have developed a dynamical model for the system, including a determination of the secondary star's rotational velocity:  $V_{\text{rot}} \sin i = 112 \pm 17 \text{ km s}^{-1}$ .

AH Her is relatively bright ( $K_{2\text{MASS}} = 11.38$ ), and the unsmoothed spectrum presented in Figure 17 is the median of twelve 3 minute exposures. The spectrum of AH Her is perhaps the most unusual of the present survey. The continuum is slightly flatter than those of K dwarfs, suggesting a spectral type near M0. Given our results for SY Cnc, V426 Oph, and SS Cyg, however, this flat spectrum is probably due to accretion disk contamination, since AH Her was on its way to an outburst. All of the absorption features in the spectrum of AH Her are weaker than they should be for a late-type star, suggesting that the contamination from the accretion disk has seriously diluted the *K*-band spectrum. If we use nearby spectral lines, we find that the ratios of most strong atomic lines are consistent with a mid-K spectral type. This agrees with the result from Horne et al. (1986). However, there are a number of anomalies, such as the missing Mg I doublet at 2.106  $\mu$ m, and the Al I line at 2.116  $\mu$ m. It is probable that there is He I emission (at 2.113  $\mu$ m) that is filling in these

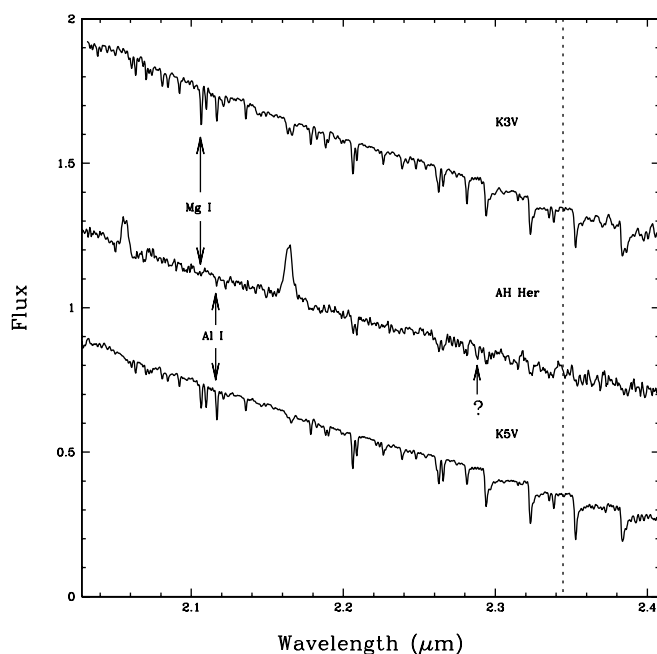


FIG. 17.—Unsmoothed spectrum of AH Her compared with K3 V and K5 V templates. The Mg I doublet at 2.106  $\mu$ m and the Al I line at 2.116  $\mu$ m are identified with arrows. Both features are very weak in the spectrum of AH Her. An unidentified absorption feature at 2.288  $\mu$ m is also marked. While the  $^{12}\text{CO}$  features for AH Her are very weak, the  $^{13}\text{CO}$  (2–0) band head at 2.345  $\mu$ m (dotted line) is clearly present.

lines, as the Mg I line at 2.281  $\mu$ m is at its proper strength (relative to the nearby Ca I triplet). At 2.288  $\mu$ m, between the Mg I line and the first overtone of CO, is an unidentified absorption feature. The entire set of  $^{12}\text{CO}$  features are very weak, at most one-half their normal strength. At the same time, however, the  $^{13}\text{CO}$  (2–0) seems to be detected! While the S/N in this region is not especially high, the Na I doublet that precedes the  $^{13}\text{CO}$  (2–0) is at a strength that is consistent with the other atomic lines in the spectrum, and the  $^{13}\text{CO}$  (2–0) is at least as strong as this doublet. New *K*-band spectra when AH Her is in quiescence would be extremely valuable for further examination of these anomalies.

## 4. DISCUSSION

There are two consistent results from our *K*-band survey of long-period cataclysmic variables. The first is that just about all of the CV systems studied here exhibit weaker than expected CO absorption features for their apparent spectral types. The other common trend is for systems with luminous accretion disks to have redder continua than expected. There are two plausible explanations for the weakness of the CO features: either carbon and/or oxygen is deficient in the secondary stars of these systems, or weak CO emission is occurring from elsewhere in the system that fills in the absorption features of the secondary star. Howell, Harrison, & Szkody (2004) have recently used Keck to obtain high-S/N observations of WZ Sge, which reveal both CO and molecular hydrogen (at 2.22  $\mu$ m) in emission. In the case of WZ Sge, the H $_2$  emission was about one-third the strength of the emission from the first-overtone band head of CO. There is no evidence of H $_2$  emission in any of the objects discussed here. Given this, and the evidence for carbon deficits seen in the UV spectra of some of the white dwarfs in CVs (e.g., U Gem), it seems more likely that carbon is underabundant in CV

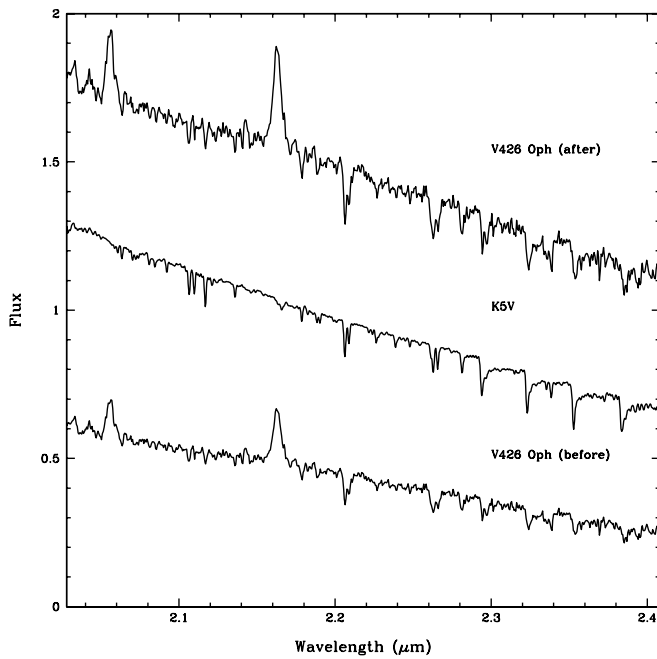


FIG. 18.—Spectrum of V426 Oph (*bottom*). This spectrum is much flatter than that of a K5 V template (*middle*), even though most of the absorption features are consistent with an early- or mid-type K dwarf. After subtraction of a contaminating source that has a flat spectrum ( $F_\lambda = \text{const}$ ) and supplies 44% of the K-band flux, the slope of the continuum of V426 Oph (*top*) now matches that of the K5 V template. Now, however, that all of the absorption features (except CO) are now much stronger than seen in a K5 V.

secondary stars. Unfortunately, because the CVs in our sample are all long-period systems with G and K dwarf secondaries, the water vapor features seen in the spectra of the M-type stars found in short-period CVs are not present, and it will be difficult to conclusively rule out an oxygen deficit for these objects using K-band spectra.

That the K-band continua of many long-period CVs appear flatter or redder than the spectra of G- and K-type secondaries can be explained by having a contaminating source that has a spectrum less steep than the  $F_\lambda \propto \lambda^{-4}$ , blackbody-like spectra of G- and K-type stars. Both the standard accretion disk spectrum ( $F_\lambda \propto \lambda^{-7/3}$ ) and free-free emission ( $F_\lambda \propto \lambda^{-2}$ ) are possible sources. To demonstrate what happens when we remove a contaminating source, we present the spectrum of V426 Oph in Figure 18, from which a flat continuum source ( $F_\lambda = \text{const}$ ), with 44% of its K-band flux, has been subtracted.

While the resulting spectrum has an identical slope to the K5 V template, the absorption lines of sodium and calcium are now too strong for a dwarf star! To achieve the same result with a free-free or accretion disk spectrum requires them to constitute an even larger fraction of the K-band flux, with the result of even stronger absorption lines. Only the subtraction of spectra with a positive spectral index can minimize this effect. We are unaware of any physical process that can generate such spectra, but observations using the *Spitzer Space Telescope* would help quantify the nature of this emission.

#### 4.1. $^{13}\text{CO}$ and Other Apparent Abundance Anomalies

The goal of our program was to investigate whether the secondary stars in long-period CVs show evidence for peculiar abundances. We summarize our results in Table 2, where a plus sign indicates a possible enhancement, and a minus a deficit (a question mark indicates uncertain, while an exclamation point indicates a significant deficit). Ellipsis dots indicate that the spectrum was either too poor or too contaminated to have confidence in statements about the abundance of a particular element. A zero indicates that a species seems to be at relatively normal level. While every single object appears to have something peculiar about its spectrum, the K-band data alone are not quite sufficient to determine the source of these peculiarities. Only for SS Cyg, RU Peg, and V426 Oph were the S/Ns of the spectra sufficiently high to confidently examine them for low-level enhancements or deficits.

Except for the near-universal weakness of CO, there is no apparent pattern in the strength of the lines from any particular element. This indicates to us that normal cosmic dispersion might be mostly responsible for the observed abundance peculiarities. Given the complex environment in which the spectrum of a CV is emitted, unusual line strengths could also arise as a result of other effects. One feature, however, does stand out: the detection of  $^{13}\text{CO}$  in four of the systems (MU Cen, EM Cyg, SS Cyg, and AH Her). In Figure 19, we show close-up views of the spectra of these four objects in the region around the  $^{13}\text{CO}$  (2–0). In the normal main-sequence counterparts of the (mostly) K-type stars found in this sample of long-period CVs, any  $^{13}\text{CO}$  absorption is almost undetectable. But we find evidence for fairly strong features in these four CVs. Even in the objects where the S/N of the spectra is quite low (e.g., CH UMa), there is evidence for  $^{13}\text{CO}$  features. *Only for RU Peg and V426 Oph can we rule out enhanced levels of  $^{13}\text{CO}$ .* In the models of Marks & Sarna (1998), the presence of  $^{13}\text{C}$  was strong evidence for evolution

TABLE 2  
APPARENT ABUNDANCE ANOMALIES

Object	Na	Mg	Al	Si	Ca	Ti	Fe	CO
V442 Cen.....	+?	+?	...	...	...	...	-?	-?
SY Cnc.....	0	0	0	-	0	0	0	0
RU Peg.....	0	0	0	-	0	0	0	-
CH UMa.....	...	...	...	...	...	...	...	-, 13+
MU Cen.....	...	...	...	+	...	...	+	-
TT Cr1.....	...	...	+?	...	-?	...	...	-!
AC Cnc.....	...	...	...	...	...	...	...	0?
EM Cyg.....	...	...	-	...	...	-	...	-, 13+
V426 Oph.....	0	0	-	0	0	0	0	-
SS Cyg.....	0	-	-?	0	0	0	0	-, 13+
BV Pup.....	...	+?	...	...	...	...	...	0
AH Her.....	...	...	?	...	...	...	...	-, 13+

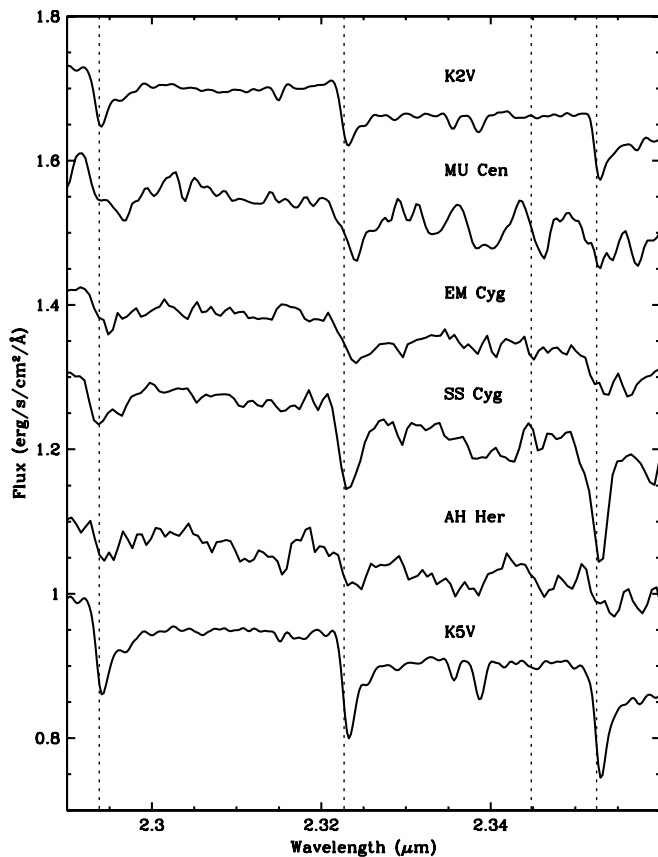


FIG. 19.—Close-up view of the spectra of MU Cen, EM Cyg, SS Cyg and AH Her showing the region of the *K* band containing the main CO features. The dotted vertical lines indicate the location of the band heads for  $^{12}\text{CO}$  (2–0) at  $2.294\ \mu\text{m}$ ,  $^{12}\text{CO}$  (3–1) at  $2.321\ \mu\text{m}$ , the  $^{13}\text{CO}$  (2–0) feature at  $2.345\ \mu\text{m}$ , and  $^{12}\text{CO}$  (4–2) at  $2.354\ \mu\text{m}$ . The *K*-band spectra of normal K2 and K5 dwarfs are plotted for comparison.

of the secondary star, resulting from the baring of, or mixing in of material from, layers where the CNO cycle had been operating. In such cases, the isotopic ratios of carbon, nitrogen, and oxygen in the photospheres of the secondary star were found to reach unusually high values. In this process, the common isotopes ( $^{12}\text{C}$ ,  $^{14}\text{N}$ , and  $^{16}\text{O}$ ) of these three species become depleted. Given that we simultaneously observe both an apparent  $^{12}\text{CO}$  depletion and  $^{13}\text{CO}$  enhancement, this suggests that material enriched from the CNO cycle is reaching the photospheres of CV secondary stars.

As described above, there are at least four presently envisioned paths that can provide CNO isotopic enrichment: (1) the accretion of CNO-processed material during the common-envelope phase, (2) the accretion of novae ejecta, (3) the possibility that the donor star originally had a higher mass than the white dwarf primary and is now the CNO-enriched core of this massive star, and (4) the secondary stars have begun to evolve off of the main sequence before becoming a CV. The first two paths are consistent with the current evolutionary paradigm for CVs, which requires the secondary stars to have undergone little evolution during their lifetimes as short-period binaries. The scenario in which the secondary stars suffer large CNO enrichment from the accretion of novae ejecta seems difficult to sustain, since the time between classical nova explosions is large ( $10^4\ \text{yr}$ ) and the amount of material that can be accreted is relatively small ( $\ll 10^{-4}\ M_{\odot}$ ). The small amount of ejecta that could be realistically accreted

would get mixed into the secondary star quickly enough to be become virtually undetectable. A similar scenario is envisaged for the common-envelope phase. The time interval between the common-envelope phase and the time of first contact of the secondary star with its Roche lobe is believed to be so long ( $>10^8\ \text{yr}$ ) that any accreted material would be thoroughly mixed into deeper layers within the secondary star.

The apparent detection of enhanced levels of  $^{13}\text{CO}$  indicates that CNO-processed material is present in the atmospheres of secondary stars of these long-period systems, and that they have either undergone some evolution off of the main sequence or they are the stripped cores of more massive stars. The main difficulty with either of these two scenarios is that population synthesis models by Howell et al. (2001) find that very few CVs are formed with high-mass secondary stars. It is interesting to note that we *do* detect at least one relatively normal CV secondary star (SY Cnc) that has a spectral type similar to that of the Sun. The possibility that there are some CV secondary stars with initial masses of over  $1\ M_{\odot}$  does not seem too far-fetched.

#### 4.2. The Case for Subgiant Secondary Stars in SS Cyg and RU Peg

In Harrison et al. (2000), an investigation into the nature of the secondary star in SS Cyg was made by combining a high-precision *HST* Fine Guidance Sensor (FGS) parallax with ground-based photometry. It was found that if all of the infrared luminosity of SS Cyg was presumed to be coming from the secondary star, then the secondary star must be a K4 subgiant. Recently, Harrison et al. (2004) reported an *HST* FGS parallax for RU Peg ( $\pi = 3.55\ \text{mas}$ ). Given that the spectrum of the secondary star in RU Peg appears uncontaminated by accretion disk emission, we thought it interesting to compare it with SS Cyg. In Figure 20, we present the spectral energy distributions of SS Cyg (data from Harrison et al. 2000) and RU Peg (data from Harrison et al. 2004). The distributions of the two systems are very similar. Their

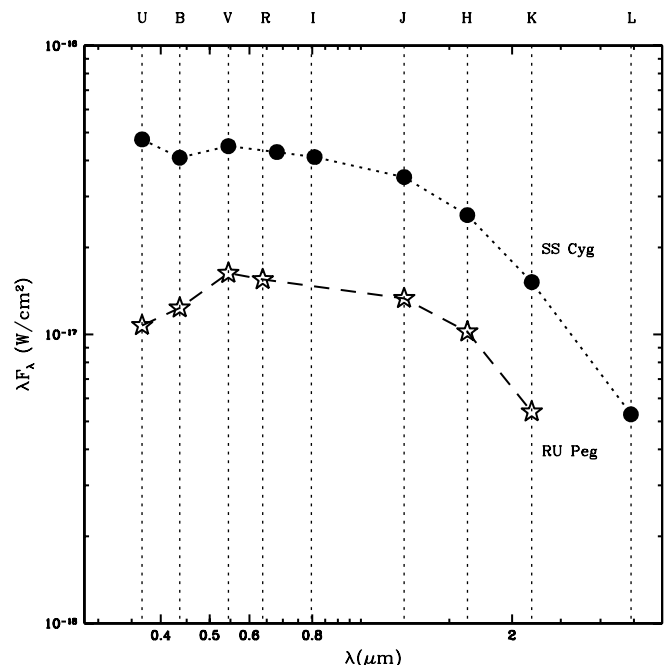


FIG. 20.—Observed spectral energy distribution for SS Cyg (circles) from Harrison et al. (2000), and for RU Peg (stars).

observed  $K$  magnitudes differ by  $\Delta K = 1.12$ , while their distance moduli differ by 1.16 mag! Thus, these two systems have nearly identical  $K$ -band luminosities:  $M_K = 3.26$  (RU Peg) and  $M_K = 3.30$  (SS Cyg). These values should be compared with a K2 V (the derived spectral type for RU Peg), which has an absolute magnitude of  $M_K = 4.15$ , while a K4 V (the spectral type for SS Cyg) has  $M_K = 4.48$ . Thus, if the entire  $K$ -band luminosities are ascribed to their secondary stars, RU Peg is 0.89 mag above the main sequence, and SS Cyg is 1.18 mag above the main sequence. It is difficult to envision a scenario in which accretion disk contamination could supply  $\approx 1$  mag of luminosity yet not severely contaminate the secondary star's spectrum. It therefore seems quite likely that both RU Peg and SS Cyg have secondary stars that have evolved off of the main sequence.

## 5. CONCLUSIONS

We have obtained moderate-resolution  $K$ -band spectra of a dozen long-period ( $P_{\text{orb}} > 6$  hr) cataclysmic variables and clearly detect the secondary stars in every system. We find weaker than normal  $^{12}\text{CO}$  absorption in nearly every object. There is evidence for enhancements or deficits for other elements, but for the most part, the spectra lack sufficient S/N to make conclusive statements. Higher S/N data are clearly needed but will require 8 and 10 m telescopes. In addition, it would be extremely useful to have somewhat higher resolution

data in order to carefully examine the CO features to determine whether there is low-level CO emission occurring that might create the false appearance of weak absorption features. Mid-infrared photometry, such as provided by *Spitzer*, would help unravel the redder than expected continua, allowing us to deconvolve, and remove, the contaminating flux from the spectra of systems with luminous accretion disks.

This research was performed with funding from National Science Foundation grant AST 99-86823, which provided partial support for T. E. H.; H. L. O. acknowledges support from a New Mexico Space Grant Consortium fellowship. This research has made use of the NASA/IPAC Infrared Science Archive, which is operated by the Jet Propulsion Laboratory, California Institute of Technology, under contract with the National Aeronautics and Space Administration. This publication also makes use of data products from the Two Micron All Sky Survey, which is a joint product of the University of Massachusetts and the Infrared Processing and Analysis Center/California Institute of Technology, funded by the National Aeronautics and Space Administration and the National Science Foundation. We would also like to acknowledge use of the AAVSO's on-line data archive to examine the outburst states of the program CVs.

## REFERENCES

- Bianchini, A., Skidmore, W., Bailey, J. M., Howell, S., & Canerna, R. 2001, *A&A*, 367, 588
- Cheng, F.-H., Sion, E. M., Szkody, P., & Huang, M. 1997, *ApJ*, 484, L149
- Dhillon, V. S., & Marsh, T. R. 1995, *MNRAS*, 275, 89
- Downes, R. A., Webbink, R. F., Shara, M. M., Ritter, H., Kolb, U., & Duerbeck, H. W. 2001, *PASP*, 113, 764
- Dulude, M., & Sion, E. M. 2002, *BAAS*, 34, 1163
- Echevarría, J., Diego, F., Tapia, M., Costero, R., Ruiz, E., Salas, L., Gutiérrez, L., & Enríquez, R. 1989, *MNRAS*, 240, 975
- Friend, M. T., Martin, J. S., Cannon Smith, R., & Jones, D. H. P. 1990, *MNRAS*, 246, 654
- Gänsicke, B. T., et al. 2003, *ApJ*, 594, 443
- Harrison, T. E., Johnson, J. J., McArthur, B. E., Benedict, G. F., Szkody, P., Howell, S. B., & Gelino, D. M. 2004, *AJ*, 127, 460
- Harrison, T. E., McNamara, B. J., Szkody, P., & Gilliland, R. L. 2000, *AJ*, 120, 2649
- Hessman, F. V. 1988, *A&AS*, 72, 515
- Hinkle, K., Wallace, L., & Livingston, W. 1995, *PASP*, 107, 1042
- Horne, K., Wade, R. A., & Szkody, P. 1986, *MNRAS*, 219, 791
- Howell, S. B., Harrison, T. E., & Szkody, P. 2004, *ApJ*, 602, L49
- Howell, S. B., Nelson, L. A., & Rappaport, S. 2001, *ApJ*, 550, 897
- José, J., Coc, A., & Hernandez, M. 2001, *ApJ*, 560, 897
- Long, K., & Gilliland, R. L. 1999, *ApJ*, 511, 916
- Lyons, K., Stys, D., Slevinsky, R., Sion, E., & Wood, J. H. 2001, *AJ*, 122, 327
- Maiolino, R., Rieke, G. H., & Rieke, M. J. 1996, *AJ*, 111, 537
- Marks, P. B., & Sarna, M. J. 1998, *MNRAS*, 301, 699
- Martínez-Pais, I. G., Giovannelli, F., Rossi, C., & Gaudenzi, S. 1994, *A&A*, 291, 455
- Mennickent, R. E., & Diaz, M. P. 2002, *MNRAS*, 336, 767
- North, R. C., Marsh, T. R., Moran, C. K. J., Kolb, U., Smith, R. C., & Stehle, R. 2000, *MNRAS*, 313, 383
- Ritter, H., & Kolb, U. 1998, *A&AS*, 129, 83
- Schenker, K., King, A. R., Kolb, U., Wynn, G. A., & Zhang, Z. 2002, *MNRAS*, 337, 1105
- Schlegel, E. M., Kaitchuck, R. H., & Honeycutt, R. K. 1984, *ApJ*, 280, 235
- Sion, E. M. 1999, *PASP*, 111, 532
- Sion, E. M., Cheng, F., Godon, P., & Szkody, P. 2002, *BAAS*, 34, 1162
- Sion, E. M., Cheng, F.-H., Sparks, W. M., Szkody, P., Huang, M., & Hubeny, I. 1997, *ApJ*, 480, L17
- Sion, E. M., Cheng, F.-H., Szkody, P., Sparks, W., Gänsicke, B., Huang, M., & Mattei, J. 1998, *ApJ*, 496, 449
- Sion, E. M., Szkody, P., Gänsicke, B., Cheng, F.-H., LaDous, C., & Hassall, B. 2001, *ApJ*, 555, 834
- Stover, R. J., Robinson, E. L., & Nather, R. E. 1981, *ApJ*, 248, 696
- Szkody, P., & Feinswog, L. 1988, *ApJ*, 334, 422
- Szkody, P., Williams, R. E., Margon, B., Howell, S. B., & Mateo, M. 1992, *ApJ*, 387, 357
- Urban, J., Lyons, K., Mittal, R., Nadalin, I., DiTuro, P., & Sion, E. 2000, *PASP*, 112, 1611
- Vande Putte, D., Cannon Smith, R., Hawkins, N. A., & Martin, J. S. 2003, *MNRAS*, 342, 151
- Wallace, L., & Hinkle, K. 1997, *ApJS*, 111, 445
- Wallace, L., Livingston, W., Hinkle, K., & Bernath, P. 1996, *ApJS*, 106, 165
- Warner, B. 1995, *Cataclysmic Variable Stars* (Cambridge: Cambridge Univ. Press)